ACTA ONCOLOGICA, 2017
http://dx.doi.org/10.1080/0284186X.2017.1299218

Taylor & Francis
Taylor & Francis Group

ORIGINAL ARTICLE

Model-based approach for quantitative estimates of skin, heart, and lung toxicity risk for left-side photon and proton irradiation after breast-conserving surgery

Q5 Francesco Tommasino[a,b], Marco Durante[b], Vittoria D'Avino[c,d], Raffaele Liuzzi[c], Manuel Conson[e], Paolo Farace[f], Giuseppe Palma[c,d], Marco Schwarz[b,f], Laura Cella[c,d]* and Roberto Pacelli[d]*

[a]Department of Physics, University of Trento, Povo, Italy; [b]Trento Institute for Fundamental Physics and Applications (TIFPA), National Institute for Nuclear Physics, (INFN), Povo, Italy; [c]Institute of Biostructures and Bioimaging, National Research Council (CNR), Naples, Italy; [d]Department of Naples, National Institute for Nuclear physics (INFN), Naples, Italy; [e]Department of Advanced Biomedical Sciences, Federico II University School of Medicine, Naples, Italy; [f]Department of Protontherapy, Azienda Provinciale per I Servizi Sanitari (APSS), Trento, Italy

Q1

ABSTRACT

Background: Proton beam therapy represents a promising modality for left-side breast cancer (BC) treatment, but concerns have been raised about skin toxicity and poor cosmesis. The aim of this study is to apply skin normal tissue complication probability (NTCP) model for intensity modulated proton therapy (IMPT) optimization in left-side BC.

Material and methods: Ten left-side BC patients undergoing photon irradiation after breast-conserving surgery were randomly selected from our clinical database. Intensity modulated photon (IMRT) and IMPT plans were calculated with iso-tumor-coverage criteria and according to RTOG 1005 guidelines. Proton plans were computed with and without skin optimization. Published NTCP models were employed to estimate the risk of different toxicity endpoints for skin, lung, heart and its substructures.

Results: Acute skin NTCP evaluation suggests a lower toxicity level with IMPT compared to IMRT when the skin is included in proton optimization strategy (0.1% versus 1.7%, $p < 0.001$). Dosimetric results show that, with the same level of tumor coverage, IMPT attains significant heart and lung dose sparing compared with IMRT. By NTCP model-based analysis, an overall reduction in the cardiopulmonary toxicity risk prediction can be observed for all IMPT compared to IMRT plans: the relative risk reduction from protons varies between 0.1 and 0.7 depending on the considered toxicity endpoint.

Conclusions: Our analysis suggests that IMPT might be safely applied without increasing the risk of severe acute radiation induced skin toxicity. The quantitative risk estimates also support the potential clinical benefits of IMPT for left-side BC irradiation due to lower risk of cardiac and pulmonary morbidity. The applied approach might be relevant on the long term for the setup of cost-effectiveness evaluation strategies based on NTCP predictions.

ARTICLE HISTORY
Received 27 July 2016
Revised 15 February 2017
Accepted 18 February 2017

Introduction

The interest in proton beam therapy (PBT) for the treatment of breast cancer (BC) has substantially increased in the radiation therapy (RT) community over recent years. [1]. Taking into account the good survival obtained with photon RT for BC patients (estimated overall 5-year survival of about 89% [2]), the main motivation for the use of protons lies in the potential reduction of radiation-induced side effects such as cardiac toxicity risks which is higher for left-side BC patients [3]. Indeed, PBT delivers the lowest mean heart dose (MHD) when compared with any other photon technique, including breathing control [3,4].

A recently published study suggested that PBT is cost-effective in patients with $\geq$1 cardiac risk factors when photon radiation therapy is unable to achieve a MHD$<$5 Gy [5]. However, in their study, Darby et al. [6] reported a no-threshold linear increase of 7.4% per Gy MHD in the rate of major coronary events. The description of normal tissue complication risks for thoracic malignancies is further complicated by the reported relation between the dose released to heart and lung and cardiopulmonary complications [7,8].

Radiation induced skin toxicity (RIST) is another important end point impacting on patient quality of life. While in photon RT the skin-sparing effect is due to the initial dose build-up, this is not the case for PBT where the skin lies in the dose profile plateau region. The risks of a potential increase in RIST have long been considered a potential limiting factor in the clinical use of protons for BC treatments. A recently published review by Verma et al. showed that, according to the limited number of available clinical data, the risk of acute skin toxicities for PBT might be similar to that observed after conventional RT or even lower [9]. Those reported clinical data were mainly obtained by means of passive scattering PBT. Nowadays with proton pencil beam scanning (PBS)

CONTACT Laura Cella laura.cella@cnr.it Institute of Biostructures and Bioimaging, National Council of Research (CNR), Via T De Amicis, 80145 Naples, Italy
*These authors contributed equally to this work.

Supplemental data for this article can be accessed here.

becoming more accessible, a reduction can be expected in the dose released to the skin as a consequence of higher flexibility and enhanced modulation capability in treatment planning.

In this work, we apply a recently developed skin normal tissue complication probability (NTCP) model [10] to guide proton PBS treatment plan optimization for left-side BC. In parallel, we present a quantification of cardio-pulmonary toxicity risks after photon and proton RT based on published NTCP models. For 10 left-side BC patients, treatment plans were generated by intensity-modulated proton therapy (IMPT) techniques as well as by intensity-modulated radiation therapy (IMRT). In the long term, this approach might be relevant for the setup of cost-effectiveness evaluation based not only on dosimetric parameters but also on NTCP predictions.

Methods and material

Patients and treatments

Ten left-side localized BC cancer patients undergoing postoperative RT after conserving surgery were randomly extracted from our clinical database. Target and organs-at-risk (OARs) structures were contoured on free-breathing CT images, according to the RTOG-1005 [11] and heart contouring guidelines [12]. Left ventricle and left anterior descending (LAD) artery were also contoured. Prescription dose was 50 Gy in 2 Gy daily fractions to the planning target volume (PTV) for all patients. PTV was restricted to the whole breast. Each patient was replanned by IMPT technique. IMRT plans were also generated as benchmark. Plan acceptance criteria were defined according to RTOG-1005 guidelines (details in Supplementary Table S1). Dose to LAD was not included per protocol as constraint. Plans were considered acceptable if at least 95% of PTV received at least 90% of prescription dose.

IMPT treatment planning was generated using Raystation 4.7 (RaySearch Laboratories, Stockholm, Sweden) with pencil beam dose algorithm and with a dose grid of $0.2 \times 0.2 \times 0.2\,cm^3$/voxel. Biological dose (i.e. physical dose $\times$ relative biological effectiveness [RBE]) was calculated assuming a constant RBE of 1.1. Two different beam arrangements were adopted: single frontal beam at 30° (single field optimization [SFO-IMPT] [13]) and three different beams at 30° and 30°±45° (multi-field optimization [MFO-IMPT] [14]). The beams had energies from 70 to 170 MeV (range in water, 4.1–19.5 cm). A range shifter (water equivalent thickness, 4 cm) was included in the calculations for all beams in all treatment plans.

Both SFO and MFO setups were calculated with and without including a skin-like structure in the cost-function. This structure is a layer of 3 mm depth (the order of magnitude of mean skin thickness) starting from the External ROI and following the extension of the PTV (Supplementary Materials Figure S1). In a first step, IMPT plans were calculated assuming as objectives in the cost function only the uniform dose corresponding to the prescribed 50 Gy and a minimum/maximum dose of 50/52 Gy, respectively, together with a user-defined dose fall-off. The skin-like structure was then included as an objective in the optimization with a maximum dose of 30 Gy. This dose value was selected on the basis of our previously reported acute RIST analysis where we found the skin surface receiving $\geq$30 Gy to be a predictive parameter for grade 3 toxicity [10]. Increasing the weight for the skin-objective in the cost function led to a gradual loss of PTV coverage. Thus, this weight was increased only up to the point when the above acceptability criteria for PTV coverage were satisfied.

IMRT plans were generated using the direct machine parameter optimization (DMPO) technique and collapsed cone convolution (CCC) algorithm implemented in the treatment planning system (TPS) Pinnacle 9.10 (Philips Medical Systems, Cleveland, OH) setting a dose grid of $0.1 \times 0.1 \times 0.1\,cm^3$/voxel. Photon treatments were based on the delivery of two tangential IMRT DMPO 6 MV beams [15]. Two additional non-tangential (anterior-oblique) IMRT beams were used if needed to satisfy constraint criteria as suggested by Farace et al. [16]. More information about the IMRT technique is included in the Supplementary Materials section.

Dosimetric analysis

For each patient, relevant DVH metrics were analyzed: the percentage volume receiving at least x dose (V_x), near maximum dose ($D_{2\%}$), near minimum dose ($D_{98\%}$), mean dose (D_{mean}), and median dose (D_{med}).

Dose surface histogram (DSH) of the body was considered representative of skin irradiation [10]. The dose in the high-dose region was assessed via the conformity index ($CI = V_{95\%}/PTV_{vol}$) and the homogeneity index ($HI = [D_{2\%} - D_{98\%}]/D_{med}$).

Normal tissue complication probability and statistical analysis

Toxicity risks were calculated according to several NTCP models available in the literature (details in Table 1). Briefly, Lyman–Kutcher–Burman (LKB), logistic, and multivariable logistic models (MVL) were employed [6,10,17–19]. Severe acute RIST was estimated starting from relative DSH [10]. To this end, for each patient DSH were normalized by the skin surface receiving at least 0.5 Gy in the photon plan (irradiated breast region). Of note, when available, NTCP models specifically extrapolated from breast cancer patients' cohorts were used [6,10,17].

The relative risk ($RR = NTCP_{protons}/NTCP_{photons}$) ratios for the different proton plans compared to photons were also calculated.

The median and the range were employed to describe all continuous variables and the non-parametric Anova (Friedman matched-pairs signed-rank test) was used to determine any significant statistical differences ($p < 0.05$). A post-hoc procedure was performed in order to identify significant differences between groups (Dunn's test).

Results

The best PTV coverage in our study was obtained by both SFO and MFO-IMPT (Figure 1(A) and Table 2) with the skin not included in the optimization ($CI = 0.99$, $HI = 0.05$).

Table 1. Organs at risk, corresponding clinical endpoints, and normal tissue complication probability (NTCP) models used in the present work.

Organ at risk	Clinical endpoint	Reference	Model
Left ventricle	Heart valvular defect	Cella et al. (2013) [19]	Logistic model: NTCP $=1/(1+e^{-S})$ $S=0.0346\times$ left ventricle V_{30} (%) $+0.0366\times$ left ventricle volume (cc)$-0.0018\times$ lung volume (cc)-2.26
	Cardiac perfusion defect	Das et al. (2005) [17]	LKB model: $TD_{50}=29$ Gy, $m=0.41$, $n=0.16$
LAD	Coronary stenosis	Moignier et al. (2015) [18]	Logistic model: (OR)$\circ D_{med}$ OR $=1.049$
Heart	Major coronary events	Darby et al. (2013) [6]	Linear model: $B_s\times(1+\mathrm{KD})$ D dose in Gy, $K=0.074$/Gy
Left lung	Radiation fibrosis	Cella et al. (2015) [7]	Logistic model: NTCP $=1/(1+e^{-S})$ $S=0.062\times$ age $(y)+0.026\times$ heart M_{30} (%) $+0.027\times$ left lung V_5 (%)-5.51
Skin (breast region body surface)	Severe acute toxicity	Pastore et al. (2016) [10]	LKB model: $TD_{50}=39$ Gy, $m=0.14$, $n=0.38$

LKB: Lyman–Kutcher–Burman; OR: odds ratio; V_X: percentage volume exceeding $\times$ Gy; D_{med}: median dose; B_S: risk of coronary events without RT; M_X: percentage mass exceeding $\times$ Gy; TD_{50}: tolerance dose that results in 50% complication probability.

COLOR Online / B&W in Print

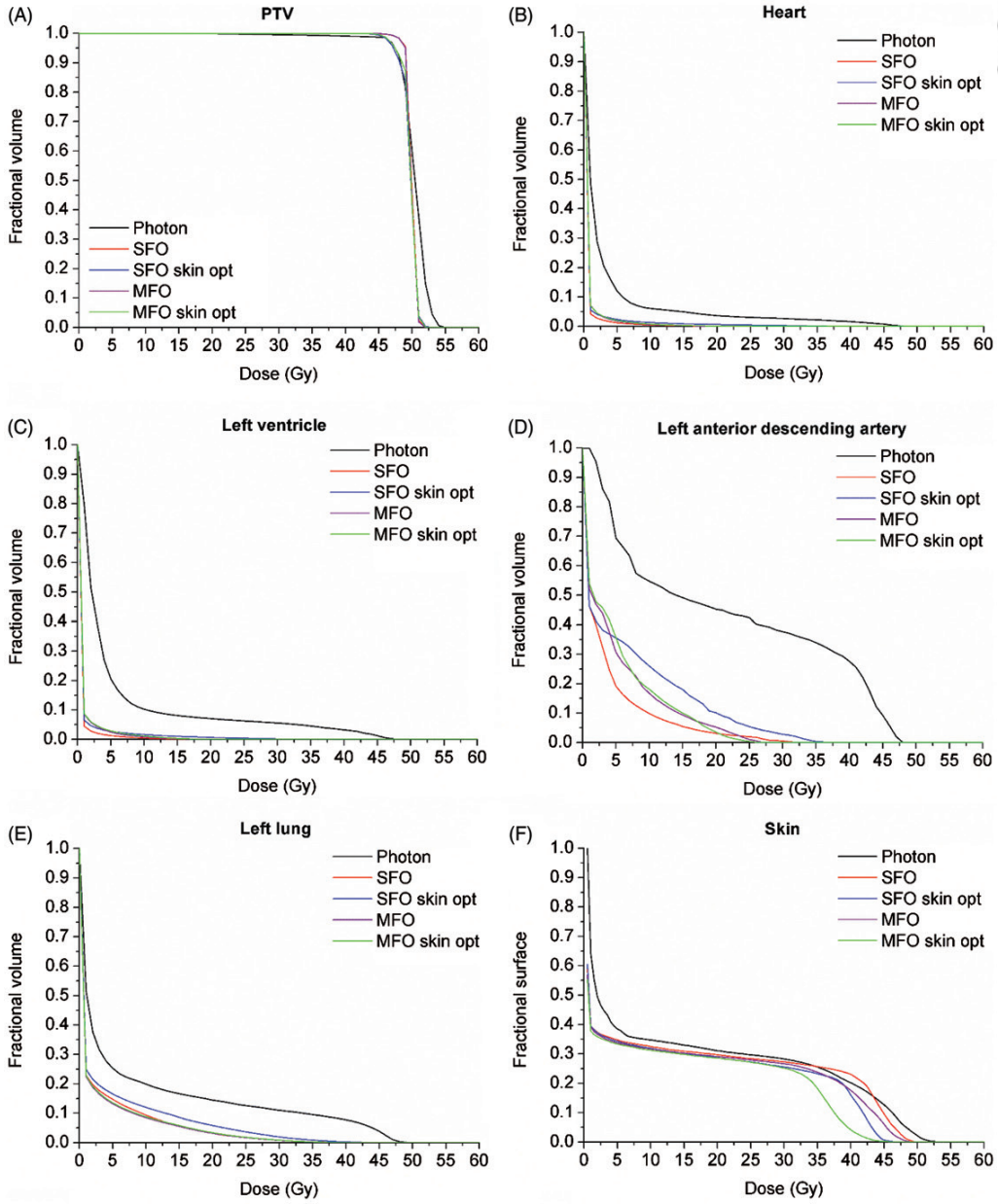

Figure 1. Median cumulative patient dose-volume histograms (DVHs) for the PTV (A), the organs-at-risk (B–E) and median cumulative patient dose–surface histogram (DSH) for the skin (F).

Table 2. Dosimetric parameters and comparative analysis for different organs for photon and proton plans.

	Photon Plan	Proton plan				p value <0.05[a]	
		Median (range)					
	IMRT a	SFO 1	SFO skin optimized 2	MFO 3	MFO skin optimized 4	Proton versus photon	Proton versus proton
PTV **coverage**							
CI	0.9 (0.7–1.0)	1.0 (1.0–1.0)	0.9 (0.9–1.0)	1.0 (1.0–1.0)	0.9 (0.9–1.0)	a ≠1, 3	1 ≠ 2,4; 2 ≠ 3; 3 ≠ 4
HI	0.1 (0.1–0.3)	0.1 (0.0–0.1)	0.1 (0.0–0.1)	0.1 (0.0–0.1)	0.1 (0.1–0.1)	a ≠1– 4	1 ≠ 2,4; 2 ≠ 3; 3 ≠ 4
Heart							
V_{20} (%)	3.6 (2.9–5.0)	0.1 (0.0–1.1)	0.6 (0.0–2.0)	0.1 (0.0–1.4)	0.1 (0.0–1.3)	a ≠1–4	1 ≠ 2,4; 2 ≠ 4; 3 ≠ 2,4
D_{mean} (Gy)	3.5 (2.6–3.9)	0.3 (0.2–0.8)	0.5 (0.3–1.2)	0.4 (0.3–1.2)	0.4 (0.3–1.2)	a ≠1–4	1 ≠ 2–4
Left **ventricle**							
V_{30} (%)	5.5 (0.0–9.1)	0.0 (0.0–1.1)	0.1 (0.0–1.0)	0.0 (0.0–1.3)	0.0 (0.0–0.6)	a ≠1–4	1 ≠ 2; 2 ≠ 3,4
D_{mean} (Gy)	5.5 (4.1–6.9)	0.3 (0.1–1.1)	0.6 (0.1–1.2)	0.5 (0.1–1.6)	0.5 (0.1–1.6)	a ≠1–4	1 ≠ 2–4; 3 ≠ 4
LAD							
D_{med} (Gy)	13.5 (5.5–31.3)	0.6 (0.0–6.4)	0.7 (0.5–9.3)	1.4 (0.8–10.9)	1.6 (0.7–10.8)	a ≠1–4	1 ≠ 2–4; 2 ≠ 4; 3 ≠ 4
Left lung							
V_{20} (%)	14.4 (10.2–16.9)	3.1 (1.1–6.2)	5.8 (1.3–9.2)	3.1 (1.0–7.6)	3.4 (1.0–5.6)	a ≠1–4	1 ≠ 3; 2 ≠ 1–4; 3 ≠ 2
D_{mean} (Gy)	7.6 (5.8–10.5)	2.6 (0.9–3.3)	3.3 (1.6–4.5)	2.5 (1.1–3.7)	2.5 (1.2–3.2)	a ≠1–4	1 ≠ 2; 2 ≠ 3,4
Skin							
S_{30} (%)	28.3 (19.0–31.1)	27.3 (19.4–29.4)	25.6 (18.7–28.3)	26.7 (18.4–29.7)	25.2 (17.4–28.6)	a ≠2,4	1 ≠ 2,4; 2 ≠ 4; 3 ≠ 4
D_{mean} (Gy)	14.9 (11.4–16.3)	13.50 (9.7–14.7)	12.24 (8.9–13.7)	12.4 (9.1–14.5)	11.1 (8.0–12.8)	a ≠1–4	1 ≠ 2–4; 2 ≠ 4; 3 ≠ 4

SFO: single field optimization; MFO: multi-field optimization; D_{max}: maximum dose; D_{mean}: mean dose; D_{med}: median dose; V_X: percentage volume exceeding × Gy, S_x: percentage surface exceeding × Gy; LAD: left anterior descending coronary artery.
[a]Friedman test plus post-hoc analysis (Dunn test) for multiple comparison between plans: proton plans significantly different from the photon plan (first column), couples of significantly different proton plans (second column).

Table 3. Normal tissue complication probability (NTCP) or odds ratio (or) values and comparative analysis for different organs and endpoints for photon and proton plans.

	Photon plan	Proton plan				p value <0.05[a]	
		Median (range)					
	IMRT a	SFO 1	SFO skin optimized 2	MFO 3	MFO skin optimized 4	Photon versus proton	Proton versus proton
	NTCP (%)						
Left ventricle							
Heart valvular defect	20.5 (8.3–93.9)	18.1 (6.5–92.6)	18.2 (6.5–92.6)	18.1 (6.5–92.6)	18.1 (6.5–92.6)	a ≠1–4	1 ≠ 2; 2 ≠ 3,4
Cardiac perfusion defect	33.8 (16.7–38.4)	3.7 (2.4–18.1)	10.6 (2.7–21.1)	3.8 (2.0–17.0)	4.1 (1.8–12.7)	a ≠1–4	1 ≠ 2; 2 ≠ 3,4
Heart							
MCE[b]	2.0 (1.9–2.1)	1.6 (1.6–1.7)	1.7 (1.6–1.7)	1.6 (1.6–1.7)	1.6 (1.6–1.7)	a ≠1–4	1 ≠ 2–4
Left lung							
Radiation fibrosis[c]	20.8 (18.5–35.4)	15.5 (12.3–16.3)	16.2 (13.5–18.4)	14.9 (12.7–16.6)	15.0 (12.8–16.7)	a ≠1–4	1 ≠ 2,3; 2 ≠ 3,4
Skin							
Severe acute toxicity	1.7 (0.3–3.2)	1.4 (0.2–2.7)	0.5 (0.1–0.9)	0.7 (0.1–2.5)	0.1 (0.0–0.5)	a ≠2–4	1 ≠ 2–4; 2 ≠ 3,4; 3 ≠ 4
dose reduced by 10%	0.4 (0.1–0.9)	–	–	–	–	a ≠1,3,4	1 ≠ 2–4; 2 ≠ 3,4; 3 ≠ 4
	OR						
LAD							
Coronary stenosis	1.9 (1.3–6.7)	1.0 (1.0–1.4)	1.0 (1.0–1.6)	1.1 (1.0–1.7)	1.1 (1.0–1.7)	a ≠1–4	1 ≠ 2–4; 2 ≠ 4

SFO: single field optimization; MFO: multi-field optimization; LAD: left anterior descending coronary artery; MCE: major coronary events.
[a]As in Table 2.
[b]Computed assuming an age of 50 years at time of irradiation and an attained age of 70 years (B_S: risk of coronary events without RT = 1.6% [6]).
[c]Computed assuming an age of 50 years at time of irradiation.

When the skin was considered in the optimization, the PTV coverage in proton plans was comparable to that of photons.

Protons generally allowed to reduce the surface receiving doses higher than 30 Gy (Figure 1(F)). The reduction was statistically significant when skin was included in the optimization ($S_{30}^{photon} = 28\%$ versus $S_{30}^{protonSF\circ} = 26\%$ or $S_{30}^{protonMF\circ} = 25\%$). The values of mean skin dose reported in Table 2 indicate a reduction of about 4 Gy between IMRT (worst case) and IMPT with skin optimization (best case).

Protons always offered statistically significant OAR dose sparing (Figure 1(B–E) and Table 2). In particular, a general reduction by about a factor of 10 in the heart and cardiac substructure mean dose was observed when using protons independently of the specific IMPT plan. At the same time, a reduction by about a factor of 3 was obtained in the case of left lung mean dose. Our analysis also showed that the specific IMPT configuration adopted did not influence dose sparing for heart and lung.

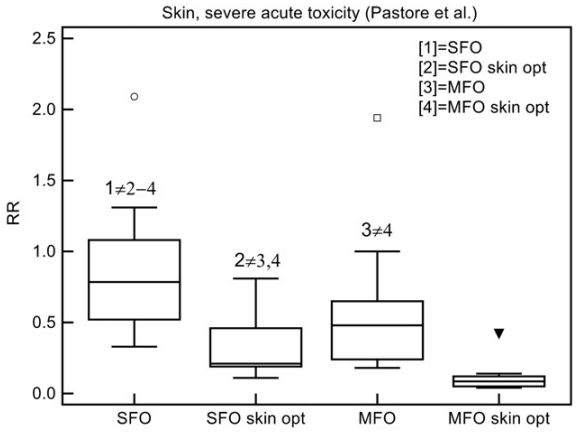

Figure 2. Relative risk (RR) ratio comparison according to normal tissue complication probability (NTCP) analysis for acute severe skin toxicity. SFO: single field optimization; MFO: multi-field optimization; skin opt.: skin included in the cost-function.

The geometry of the irradiation field and the optimization strategy both played a relevant role in reducing the risk of severe acute RIST development (Table 3). The grade 3 skin toxicity RR is significantly reduced when comparing NTCP for SFO- (≅0.8) versus MFO-IMPT (≅0.5); the RR is further reduced when the skin is included in the optimization (SFO with skin optimization ≅0.2 and MFO with skin optimization ≅0.1) (Figure 2). Importantly, PTV coverage is maintained at a level comparable or slightly better than photons (Table 2). The application of NTCP models to cardiac and lung complications (Table 3 and Figure 3) showed an overall reduction in the toxicity risk prediction for all IMPT plans compared with IMRT plan (RR <1). Depending on the considered toxicity endpoint, the RR values ranged from 0.1 to 0.7.

Discussion

In the present study, we performed a skin-NTCP driven optimization analysis for left-side BC proton treatment plans along with a comprehensive NTCP model-based analysis aimed at quantifying the potential benefit of proton beam therapy for left-side breast cancer irradiation.

BC is one of the solid tumors for which good local control is obtained with conventional photon therapy. Therefore, there is no reason to pursue a dose escalation with PBT which can be used instead to reduce the risk of radiation-induced normal tissue complications. In this context, our planning approach was aimed at obtaining the maximum advantages from the physical selectivity of IMPT in terms of OARs sparing, while keeping a PTV coverage consistent with a similar expected tumor control. This might have an impact especially for left-side BC patients.

The different toxicity end-points we considered reflect the fact that a quantification of NTCP can actually provide the link between physical dose distributions and expected clinical outcomes. This is consistent with and supportive of the so-called model-based approach for radiotherapy patient selection [20].

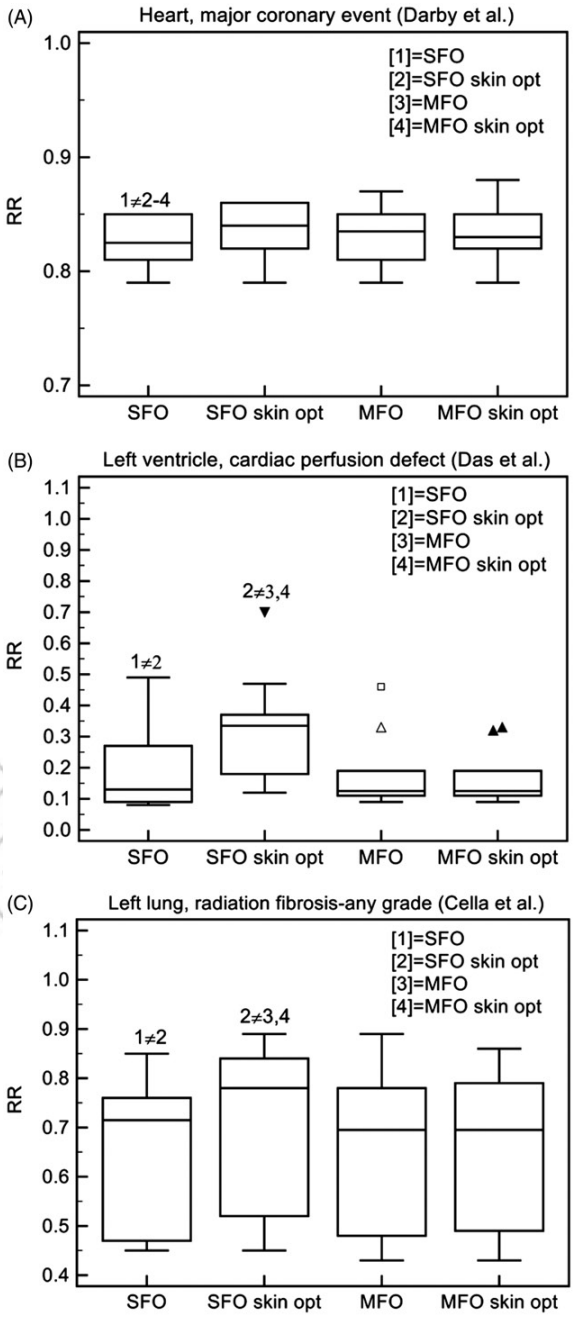

Figure 3. Relative risk (RR) ratio comparison according to normal tissue complication probability (NTCP) analysis for heart and lung. SFO: single field optimization; MFO: multi-field optimization; skin opt.: skin included in the cost-function.

To the best of our knowledge, this is the first work that evaluates the risk of radiation-induced skin toxicity in PBT. Our results show that RIST after proton irradiation could be dependent on the beam setup as well as on the optimization strategy. The RR ratios obtained for the skin suggest that a toxicity comparable with photon RT, or even lower, is expected, according to the conclusion of a recent review on clinical outcomes of PBT for breast cancer [9]. Moreover, the data in Figure 2 show that the risk of RIST is reduced by adopting MFO compared with SFO (by a factor of 2) and that including the skin into the optimization allows the

modulation of superficial dose for both proton setup, for which, therefore, an additional benefit is expected (by a factor of about 4). Skin sparing with IMPT is obtained at the expense of a limited loss in terms of PTV coverage which anyway is kept above acceptable variation levels as recommended by RTOG-1005 guidelines. Of note, the skin NTCP for photons resulting from our analysis is consistent with the outcomes of clinical studies where IMRT was associated with reduced acute grade 3 skin toxicity compared to conventional wedge-based radiation for BC treatment [21]. To our knowledge, the possibility to include the skin in PBT optimization was considered up to now only in the work recently presented by Depauw et al. [22]. However, in that case the analysis did not include the evaluation of NTCP, nor did it investigate the potential of skin optimization with different field setups. Finally, the comparison with photon data was also lacking.

The accuracy in calculating surface skin doses (build-up region) in tangential-like irradiation by commercial TPS photon algorithms is a critical issue. Several studies investigated the superficial dose prediction accuracy of CCC algorithm using different methods [23]. As a whole, those studies reported a tendency towards dose underestimation at depths lower than 2–6 mm. However, also assuming a superficial dose overestimation of about 10%, by the inclusion of the skin into IMPT optimization we obtain comparable (SFO) or even lower (MFO) RIST NTCP values in comparison with IMRT plan (Table 3).

Concerning cardio-pulmonary toxicity, we reported that in the case of valvular or cardiac perfusion defects (Figure 2(A,B)) a difference by a factor of 10 in MHD translates only in a 10% reduction in NTCP. Conversely, a difference by a factor of 10 in median LAD dose implies a 50% lower risk of coronary stenosis. As reported by Darby et al. [6], the factor 10 reduction observed in MHD for protons compared with photons translates into a reduced risk of major coronary events. For a 50-year-old woman with no preexisting cardiac risk factors, IMPT would decrease of about 0.4% her risk of having at least one acute coronary event before the age of 70 years, as if she never had RT (Table 3). A reduction is also observed in the NTCP values for lung toxicity. Of note, the expected risk of photon radiation-induced lung fibrosis resulting from our analysis is in line with that reported by Kubo et al. [24] in a cohort of patients irradiated with tangential fields after breast-conserving surgery.

Also, in the present planning study, no deep inspiration breath hold (DIBH) technique was used. However, as suggested by Mast et al. [4], we expect that using DIBH would reduce heart and lung doses by the same proportion in both photon and proton techniques.

It should be emphasized that in the present work we focused our analysis on results expressed in terms of median values of either dosimetric parameters or specific toxicity risks. However, in some cases, comparably large fluctuations are observed around those median values, as clearly evident from tables and from error bars in the figures. When evaluating NTCP for each single patient, this would translate into a different gain in terms of absolute NTCP values for protons compared to photons (so-called $\Delta NTCP = NTCP_{protons} - NTCP_{photons}$ [20]). These differences permit to identify those patients for whom a significant benefit is expected from using IMPT instead of photons and those for whom the best possible outcomes have already been obtained with photons. These considerations could then be combined with the outcomes of cost-effectiveness analysis [5], thus providing a robust motivation for adopting a more expensive treatment as IMPT.

An ambitious randomized clinical trial is now starting in the US (NCT02603341) aiming at clarifying the impact of PBT on cardiac toxicity. With an increasing attention in the proton therapy community toward BC, a much larger amount of toxicity data are expected in the next few years and will help improving our understanding of toxicity risks and consequently the predictive power of NTCP models.

Our analysis did not take into account the impact of a variable RBE for protons. Even though we expect RBE to have an impact mainly on the biological dose delivered at the distal edge of the fields, a consistent prediction of RBE effects is not to be excluded. This is due, on the one hand, to the different tissues involved (i.e. different α/β values, different endpoints), on the other hand, to the composition of IMPT fields, involving multiple energies with different weights. This work paves the way for further studies that include recalculations of proton plans taking into account variable RBE. Similarly, proton plans were optimized on the same PTV as photons, i.e. we did not take into explicit account potential impairments in the quality of proton plans due to range uncertainties and/or moving target issues. Both aspects have been investigated in the past by Ares and colleagues for a 3-field IMPT setup consistent with the one adopted in this study [15]. Even though they are recognized as potential sources of errors, the influence of range uncertainty and movement on breast proton plans was found to be minimal.

A potential limitation of our study is the use of photon-derived tissue NTCP models for patients treated with protons. However, NTCP models validation in patients treated with protons is hampered by the paucity of epidemiological data relative to the most modern RT delivery techniques, such as IMPT, which have only very recently started to become available, or are still lacking. Interestingly, Blanchard et al. [25] have very recently demonstrated the robustness and validity of a set of photon-derived NTCP models for head and neck cancer patients treated with proton therapy, and claimed the validity of the model-based approach as a strategy to select patients for proton therapy.

Moreover, although we selected models specifically built on breast cancer cohorts wherever possible, multivariate models developed on Hodgkin lymphoma cohorts were accepted.

In conclusion, given the small size of our sample and the design of the study, our analysis suggests that PBT might be safely applied without increasing the risk of severe acute radiation induced skin toxicity which can be even reduced provided that the skin is considered in the optimization strategy. The quantitative risk estimates also support the potential clinical benefits of IMPT for left breast cancer due to the lower risk of cardiac or pulmonary morbidity.

Disclosure statement

The authors report no conflicts of interest. The authors alone are responsible for the content and writing of this article.

Funding

This work has been partially supported by National Institute for Nuclear Physics (INFN) CSN5 Call "MoVe IT".

ORCID

Laura Cella http://orcid.org/0000-0003-0058-4029

References

[1] MacDonald SM. Proton therapy for breast cancer: getting to the heart of the matter. Int J Radiat Oncol Biol Phys. 2016;95:46–48.

[2] Bartelink H, Maingon P, Poortmans P, et al. Whole-breast irradiation with or without a boost for patients treated with breast-conserving surgery for early breast cancer: 20-year follow-up of a randomised phase 3 trial. Lancet Oncol. 2015;16:47–56.

[3] Taylor CW, Wang Z, Macaulay E, et al. Exposure of the heart in breast cancer radiotherapy: a systematic review of heart doses published during 2003–2013. Int J Radiat Oncol Biol Phys. 2015;93:845–853.

[4] Mast ME, Vredeveld EJ, Credoe HM, et al. Whole breast proton irradiation for maximal reduction of heart dose in breast cancer patients. Breast Cancer Res Treat. 2014;148:33–39.

[5] Vega RBM, Ishaq O, Raldow A, et al. Establishing cost-effective allocation of proton therapy for breast irradiation. Int J Radiat Oncol Biol Phys. 2016;95:11–18.

[6] Darby SC, Ewertz M, McGale P, et al. Risk of ischemic heart disease in women after radiotherapy for breast cancer. N Engl J Med. 2013;368:987–998.

[7] Cella L, D'avino V, Palma G, et al. Modeling the risk of radiation-induced lung fibrosis: irradiated heart tissue is as important as irradiated lung. Radiother Oncol. 2015;117:36–43.

[8] Cella L, Oh JH, Deasy JO, et al. Predicting radiation-induced valvular heart damage. Acta Oncol. 2015;54:1796–1804.

[9] Verma V, Shah C, Mehta MP. Clinical outcomes and toxicity of proton radiotherapy for breast cancer. Clin Breast Cancer 2016;16:145–154.

[10] Pastore F, Conson M, D'avino V, et al. Dose-surface analysis for prediction of severe acute radio-induced skin toxicity in breast cancer patients. Acta Oncol. 2016;55:466–473.

[11] RTOG 1005 protocol information minimize: a phase iii trial of accelerated whole breast irradiation with hypofractionation plus concurrent boost versus standard whole breast irradiation plus sequential boost for early-stage breast cancer. Available online: https://www.rtog.org/clinicaltrials/protocoltable/studydetails.aspx?study=1005.

[12] Feng M, Moran JM, Koelling T, et al. Development and validation of a heart atlas to study cardiac exposure to radiation following treatment for breast cancer. Int J Radiat Oncol Biol Phys. 2011;79:10–18.

[13] Johansson J, Isacsson U, Lindman H, et al. Node-positive left-sided breast cancer patients after breast-conserving surgery: potential outcomes of radiotherapy modalities and techniques. Radiother Oncol. 2002;65:89–98.

[14] Ares C, Khan S, MacArtain AM, et al. Postoperative proton radiotherapy for localized and locoregional breast cancer: potential for clinically relevant improvements? Int J Radiat Oncol Biol Phys. 2010;76:685–697.

[15] van Asselen B, Schwarz M, van Vliet-Vroegindeweij C, et al. Intensity-modulated radiotherapy of breast cancer using direct aperture optimization. Radiother Oncol. 2006;79:162–169.

[16] Farace P, Zucca S, Solla I, et al. Planning hybrid intensity modulated radiation therapy for whole-breast irradiation. Int J Radiat Oncol Biol Phys. 2012;84:e115–e122.

[17] Das SK, Baydush AH, Zhou S, et al. Predicting radiotherapy-induced cardiac perfusion defects. Med Phys. 2005;32:19–27.

[18] Moignier A, Broggio D, Derreumaux S, et al. Coronary stenosis risk analysis following Hodgkin lymphoma radiotherapy: a study based on patient specific artery segments dose calculation. Radiother Oncol. 2015;117:467–472.

[19] Cella L, Liuzzi R, Conson M, et al. Multivariate normal tissue complication probability modeling of heart valve dysfunction in Hodgkin lymphoma survivors. Int J Radiat Oncol Biol Phys. 2013;87:304–310.

[20] Widder J, van der Schaaf A, Lambin P, et al. The quest for evidence for proton therapy: model-based approach and precision medicine. Int J Radiat Oncol Biol Phys. 2016;95:30–36.

[21] Harsolia A, Kestin L, Grills I, et al. Intensity-modulated radiotherapy results in significant decrease in clinical toxicities compared with conventional wedge-based breast radiotherapy. Int J Radiat Oncol Biol Phys. 2007;68:1375–1380.

[22] Depauw N, Batin E, Daartz J, et al. A novel approach to postmastectomy radiation therapy using scanned proton beams. Int J Radiat Oncol Biol Phys. 2015;91:427–434.

[23] Cao Y, Yang X, Yang Z, et al. Superficial dose evaluation of four dose calculation algorithms. Radiat Phys Chem, Corrected proof, Available Online 2 March 2016. In press

[24] Kubo A, Osaki K, Kawanaka T, et al. Risk factors for radiation pneumonitis caused by whole breast irradiation following breast conserving surgery. J Med Invest. 2009;56:99–110.

[25] Blanchard P, Wong AJ, Gunn GB, et al. Toward a model-based patient selection strategy for proton therapy: external validation of photon-derived normal tissue complication probability models in a head and neck proton therapy cohort. Radiother Oncol S0167-8140:34286–4.